Experimental confirmation of the delayed Ni demagnetization in FeNi alloy

S. Jana, R. Knut, S. Muralidhar, et al.

View Online   Export Citation   CrossMark

ARTICLES YOU MAY BE INTERESTED IN

Experimental confirmation of the delayed Ni demagnetization in FeNi alloy

S. Jana,[1,a] (iD) R. Knut,[2] S. Muralidhar,[3] (iD) R. S. Malik,[2] (iD) R. Stefanuik,[2] J. Åkerman,[3] (iD) O. Karis,[2] (iD)
C. Schüßler-Langeheine,[1] (iD) and N. Pontius[1] (iD)

AFFILIATIONS

[1]Helmholtz-Zentrum Berlin für Materialien und Energie GmbH, Albert Einstein Straße 15, 12489 Berlin, Germany
[2]Department of Physics and Astronomy, Uppsala University, Box 516, 75120 Uppsala, Sweden
[3]Department of Physics, University of Gothenburg, 412 96 Gothenburg, Sweden

Note: This paper is part of the APL Special Collection on Ultrafast and Terahertz Spintronics.
[a]Author to whom correspondence should be addressed: sj.phys@gmail.com

ABSTRACT

Element-selective techniques are central for the understanding of ultrafast spin dynamics in multi-element materials, such as magnetic alloys. Recently, however, it turned out that the commonly used technique of the transverse magneto-optical Kerr effect (T-MOKE) in the extreme ultraviolet range may have issues with unwanted crosstalk between different elemental signals and energy-dependent non-linear response. This problem can be sizeable, which puts recent observations of ultrafast spin transfer from Fe to Ni sites in FeNi alloys into question. In this study, we investigate the Fe-to-Ni spin transfer in a crosstalk-free time-resolved x-ray magnetic circular dichroism (XMCD) experiment with a reliable time reference. With XMCD near the absorption maxima, we find a very similar Fe and Ni dynamics as with T-MOKE from identical samples. Considering the potential non-linearities of the T-MOKE response, such a good agreement in our findings is remarkable. Our data provide the ongoing discussion about ultrafast spin-transfer mechanisms in FeNi systems with a broader experimental basis.

Spin transfer between different inequivalent sites in magnetic materials is among the fastest manipulation of a magnetic state possible and, hence, attractive for spintronics applications. Revealing and optimizing such processes require methods that are selective to different magnetic species in the same material. Over last two decades, element resolved studies of magnetization dynamics became possible with the development of short-pulsed EUV (extreme ultraviolet) and x-ray sources. They allowed probing various intrinsic quantities, such as inter-atomic exchange interaction, inter-atomic spin transfer, spin and orbital contributions, and layer resolved dynamics.[1–15] The most commonly used techniques in this field are the transverse magneto-optical Kerr effect (T-MOKE) at EUV energies[3,4,14,15] and x-ray magnetic circular dichroism (XMCD) in the soft x-ray range,[5,6,16,17] which probe element resolved magnetization dynamics via resonant excitations from shallow and deep core levels, respectively.

Element-sensitive techniques are important when different elemental species in one magnetic system show different dynamics.[2,3,5,10–12,14,15,18,19] One very interesting recent result in this context is the delay of the demagnetization in Ni compared to that of Fe in an FeNi alloy:[2–4,11] T-MOKE studies on these alloys find Ni to demagnetize a couple of tens of femtoseconds delayed relative to Fe. This puzzling observation motivated theoretical modeling and two different explanations have been put forward: Knut et al. explain the observed delay in Permalloy (Py) and $Cu_{0.4}Py_{0.6}$ sample adopting an inhomogeneous magnon generation scheme that provides the mechanism of the angular momentum transfer to the lattice.[10] This model uses a combination of electron–phonon and electron–magnon interaction, initially proposed by Haag et al.[20] Hofherr et al.[13] explain the observed delay utilizing the optically induced spin transfer (OISTR) between the Fe and Ni sublattice. Both mechanisms describe fundamental processes in ultrafast spin manipulation in multi-element magnets and are, therefore, relevant beyond this particular effect.

Remarkably, the experimental basis for these theories turned out rather unfirm. The delay in the onset of demagnetization of Ni relative to that of Fe in $Fe_{1-x}Ni_x$ alloys has so far only been reported in experimental studies, which used EUV T-MOKE.[2–4,11] In contrast to that, first XMCD data reported no delay for the Ni demagnetization in the FeNi-alloy and substantially slower demagnetization for Fe.[7]

This apparent discrepancy is intriguing and disturbing; it might be caused by practical or fundamental limitations that both experimental techniques have but may as well have serious implications for the validity of the proposed mechanisms.

For $3d$ transition metals, T-MOKE is usually carried out at the $3p \rightarrow 3d$ ($M_{2,3}$) resonances in the EUV range and XMCD at the $2p \rightarrow 3d$ ($L_{2,3}$) resonances in the soft x-ray range. Both involve excitations into the magnetically relevant $3d$ states. While $L_{2,3}$-XMCD is directly probing the magnetic contribution to the x-ray absorption cross section, which—at least in equilibrium—was found to scale quite rigorously with the magnetization,[21–23] the relation between EUV T-MOKE signal and magnetization is more involved as it is sensitive to both the absorptive and dispersive properties of EUV photons. Recently, some of us showed that the relation between the asymmetry measured in T-MOKE and sample magnetization can be non-linear even in equilibrium.[24] The response is complex, including sign changes, and depends on both the photon energy of the probe pulse and the type of excitation of the spin system. Overall, such non-linearities may also affect the experimental observations discussed above.

Linearity becomes even more of an issue when two resonances are probed that overlap in energy. The energy distance between the $M_{2,3}$ resonances of two neighboring $3d$ metals is smaller than the energy width of each single resonance in the T-MOKE signal such that even the contributions from next-neighboring elements like Fe and Ni overlap. This may cause unwanted crosstalk between the dynamic signals from different elements. While T-MOKE asymmetry of elemental Fe is negligible at Ni-$M_{2,3}$ resonance, a sizable asymmetry of elemental Ni is present at Fe-$M_{2,3}$ resonance.[24] One can easily imagine this to cause experimental results that are difficult to interpret. Furthermore, in dynamics studies with T-MOKE, energy-dependent dynamic responses have been observed;[24] similarly also EUV-XMCD experiments have shown rather complex responses.[18,25]

Crosstalk problems can be excluded for the well-separated soft x-ray $L_{2,3}$ resonances; the energy difference between the Fe and Ni $L_{2,3}$ resonances exceeds the width of the elemental resonances by far. On the other hand, the large energy separation between resonances in the soft x-ray range causes other experimental problems. In the EUV, the proximity of resonances allows for simultaneous detection of the different resonances, thus automatically guaranteeing a common timescale. In contrast to that, all sources of soft x-ray pulses available today cover only one resonance at a time. One, therefore, must carefully reference time scales when studying effects like delayed dynamic response in one elemental subsystem.

Given this overall complexity, a referencing of one element-resolved techniques against the other appears a reasonable step toward providing a reliable experimental basis for theory. In this work, we directly compare the elemental magnetization dynamics in $Fe_{0.5}Ni_{0.5}$ utilizing both techniques for identical samples. Carefully avoiding all known sources of experimental problems, we can confirm that the delay of the Ni demagnetization is indeed intrinsic to the sample properties and that—somewhat surprisingly—both techniques even quantitatively find very similar dynamical responses.

Time resolved T-MOKE was performed at the HELIOS Laboratory, Uppsala University, Sweden.[26] A near-infrared (NIR) pump pulse of a wavelength of 800 nm (1.5 eV) and a pulse length of 35 fs, and EUV probe pulse of energies ranging between 40 and 70 eV and a pulse length of 20 fs are utilized in the T-MOKE-setup that measures the whole EUV spectra at once.[4] EUV photons are obtained via high harmonic generation with the same NIR pulse also used for pumping, thus ensuring intrinsic synchronization. The measurement geometry and measurement protocol are described in detail in Ref. 4. As depicted in Fig. 1(a), the sample was magnetized perpendicular to the scattering plane spanned by the directions of the incoming and reflected EUV photons; the polarization of the incoming EUV photons was linear and parallel to the scattering plane. In T-MOKE geometry, a change in the reflected intensity is observed upon reversal of the sample magnetization, which is utilized to probe the magnetization magnitude.

The XMCD experiments were performed at the BESSY-II Femtoslicing facility (beamline UE56/1-ZPM and DynaMaX endstation) at Helmholtz-Zentrum Berlin.[27] Elliptically polarized x-ray pulses of 100 fs temporal width are produced via femto-slicing of electron bunches by means of an intense NIR pulse (of a wavelength of 800 nm and a pulse width of 50 fs) generated in a seeded amplifier. An NIR pulse produced in a separate amplifier, synchronized with the slicing pulse, is used as pump pulse for sample excitation. The repetition rate of the pump pulse is 3 kHz and that of the probe pulse is 6 kHz such that alternatingly the signals with and without pump pulse (in the following referred to as pumped and unpumped signal, respectively) are detected. The measurement was performed in transmission geometry with the sample placed at 45° incidence angle with the x-ray beam. The magnetic field aligned parallel to the x-ray beam was inverted every 10 s to obtain the XMCD contrast. The x-ray photons transmitted through the sample were detected with an avalanche photo diode[27] [compare experimental scheme in Fig. 2(b)]. We recorded the XMCD data for the photon energies of largest XMCD contrast at both resonances. This choice of photon energy does not only provide the largest magnetic signal but also minimize the effects of potential energy shifts on our signal.

The sample, a 25 nm film of the $Fe_{0.5}Ni_{0.5}$ alloy, was deposited under identical deposition condition on Ta (3 nm)/Al (0.3 μm)/Si$_3$N$_4$ (0.2 μm) and on Ta (3 nm)/Si (1 mm) by means of magnetron sputtering technique to measure the XMCD in transmission and T-MOKE signal in reflection, respectively. The Al layer acts as a heat sink. A Ta layer of 3 nm was deposited on top of the sample to protect against oxidation. The pump fluences in both experiments were set to values on the order of 10 mJ/cm^2 such that similar demagnetization amplitudes were achieved.

In T-MOKE, the magnetic asymmetry spectrum $A(E)$ is defined as

$$A(E) = \frac{I_+(E) - I_-(E)}{I_+(E) + I_-(E)}, \qquad (1)$$

where $I_\pm(E)$ is the reflected intensity of photon of energy E for opposite magnetization directions ($\pm M$). As pointed out in Ref. 24, the relation between asymmetry and magnetization in T-MOKE is energy dependent. Here, we follow the standard protocol and probe the magnetization dynamics from measuring the asymmetry at energies that corresponds to the harmonics with peak asymmetries near the $M_{2,3}$ edges of Fe and Ni. The inset of Fig. 1(b) shows the difference and asymmetry spectrum. The strong shaded peaks correspond to the $M_{2,3}$ edges of Fe (near 54 eV) and Ni (near 66 eV) as indicated by arrows. We note the complex energy dependence with a sign change in between the Fe and Ni resonance maxima.
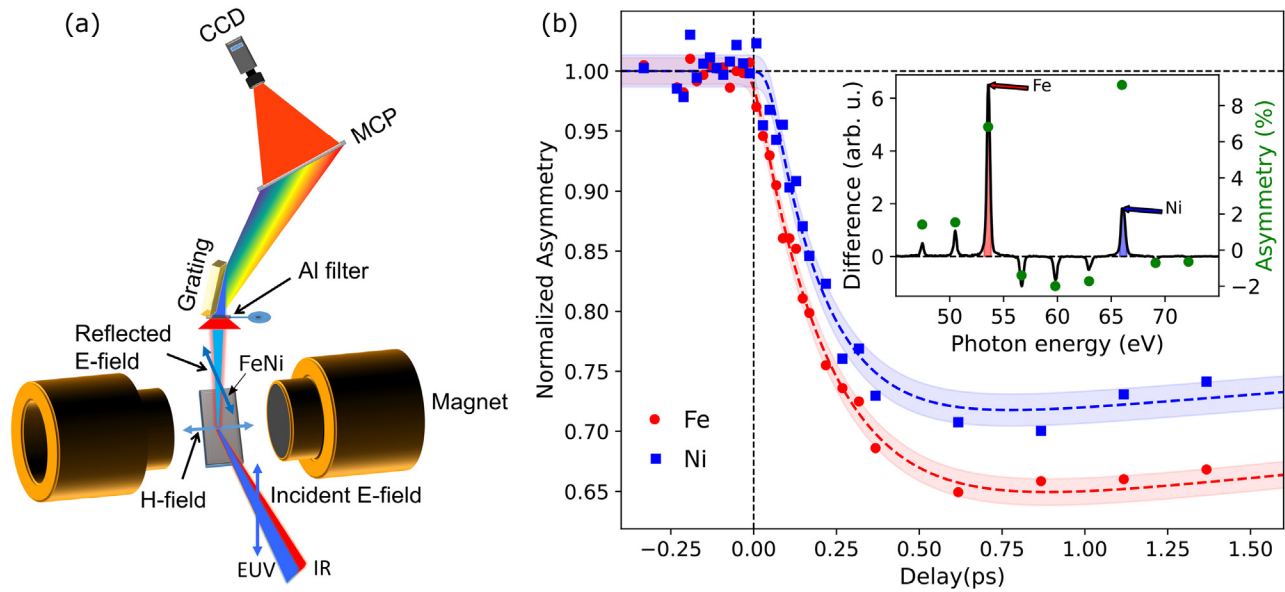
FIG. 1. (a) Scheme of the T-MOKE setup. The sample is placed at 45° incident angle and magnetized in the plane. The blue arrows indicate the EUV-polarization and the static external magnetic field. The EUV and IR photon beams are focused on the sample with nearly co-linear wave fronts. The reflected beams passes through an Al-filter to remove the pump (IR) pulse. The probe (EUV) is dispersed by a grating onto an MCP-CCD based detector. (b) Magnetization dynamics of Fe and Ni. The inset shows the static difference spectrum (black line, left axis) and the asymmetry spectrum (green symbols, right axis) obtained from the reflection spectra (see Eqn. 1). The elemental demagnetization is obtained from the peak intensity of the asymmetries near 54 and 66 eV (as depicted by red and blue regions in the inset) corresponding to the Fe (red circles) and Ni (blue squares) $M_{2,3}$ edges, respectively. The dashed lines are the fits to the experimental data. The shades have widths of $\pm$ one standard deviation of the data points estimated from the scatter of data at negative delays.

To determine the element-resolved magnetization dynamics, asymmetry spectra were recorded with different pump-probe delays. The asymmetry was normalized to one at negative pump-probe delays; the resulting asymmetry curves are plotted against the delay in the main panel of Fig. 1(b), which then represent the element resolved T-MOKE dynamics at these edges.

As the whole $A(E)$ spectrum is measured at each delay, the dynamics at Fe and Ni sites are probed simultaneously. A delay in the
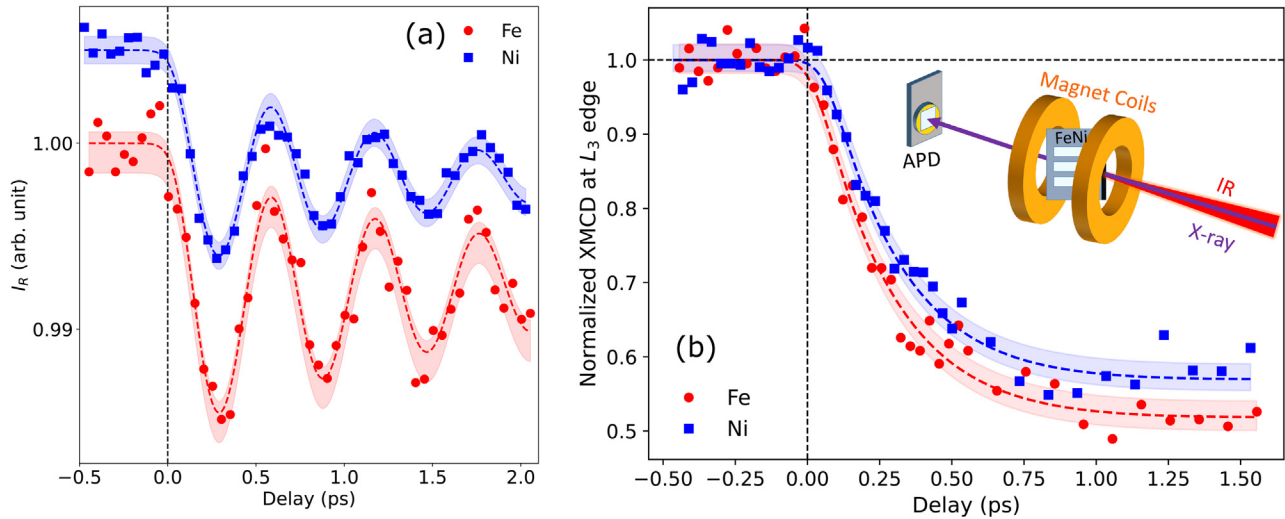

FIG. 2. (a) Oscillations of the super-lattice Bragg peak intensity from the MoSi-multilayer at the Fe (red circles) and the Ni (blue squares) L_3 energies. The Ni data are shifted upward by 0.5% for clarity. Dashed curves are fits of a damped cosine function (see the text and the supplementary material). (b) XMCD signal vs pump-probe delay measured at the Fe (red circles) and the Ni (blue squares) L_3 edges. The delay-axis of each scan is adjusted with respect to the time-reference given by the MoSi cross-correlator. The red and the blue dashed curves are fits to all measured data (see the text). The shades have widths of $\pm$ one standard deviation of the data points estimated from the scatter of points at negative delays.

onset of Ni demagnetization to that of the Fe is evident from the data. A double exponential decay function fits both the curves featuring an exponential decay and a subsequent recovery,

$$m(t) = m_0 \left[1 - m_d \left\{ 1 - \exp\left(-(t - t_s)/t_d\right) \right\} \right.$$
$$\left. \times \exp\left(-(t - t_s)/t_r\right) \right] \otimes G. \qquad (2)$$

Here, $m(t)$ is the time-dependent magnetic contrast (MC), m_0 is the initial full MC, m_d is the maximum portion of the quenched MC after excitation, t_s defines the onset of the demagnetization, while t_d and t_r are the time constants of the decay and recovery, respectively. A convolution with a Gaussian, G, with FWHM of 50 fs accounts for the experimental resolution. The results for the most relevant parameters are presented in Table I. Without loss of generality, t_s for the Fe is defined as zero. t_s for Ni is, hence, the relative delay with respect to Fe. The amount of demagnetization (m_d) of Fe is ~27% more than that of Ni. The demagnetization time constant, t_d, for Fe is by ~29% larger than that for Ni, leaving the quenching rate, m_d/t_d about the same for both the elements. A relative delay of 45 ± 9 fs in the Ni demagnetization is obtained from the fitting.

We now compare these results to the Femtoslicing L_3 XMCD data at the photon energy of the maximum XMCD effect at the Fe and Ni L_3 resonances, respectively. Here, unlike the T-MOKE setup, the element resolved magnetization cannot be measured simultaneously as the energy distance between the Fe and Ni L_3 resonances is larger than the x-ray bandwidth. Element specific information, hence, requires separate, sequential measurements at each elemental resonance. While the used femto-slicing setup has an intrinsic synchronization between pump and probe pulses, slow drifts may still occur due to, e.g., temperature changes affecting the relative beam path lengths. To ensure that the Fe and Ni dynamics is probed on identical delay scale, we used an x-ray-optical-cross-correlator (XOCC) as unique time reference.[29] This cross correlator records the laser-excited displacive coherent phonon oscillation of a MoSi multilayer structure through the first-order super-lattice Bragg reflection [Fig. 2(a)]. The time of laser excitation has a defined reference to the phase of the displacive oscillation allowing to properly align delay scales of both L_3-edge measurements with each other. Detail of the XOCC setup can be found in Refs. 28 and 29 and in the supplementary material. We implemented a measurement protocol hourly changing data acquisition between the sample and XOCC. The delay-axis for each XMCD scan was adjusted to the time reference from the MoSi XOCC by assuming a linear drift of the delay scale in between (see the supplementary material).

The such obtained time-resolved XMCD data are shown in Fig. 2(b). A delay of the Ni demagnetization compared to that of Fe is

clearly visible. For quantitative analysis, we fitted the magnetization transients of Fe and Ni with the same function as for the T-MOKE data [Eq. (2)]. The FWHM for G was set to 130 fs to account for the overall temporal resolution of the pump-probe setup. The red and the blue curves are fits to the data; the red and blue symbols are obtained by averaging over all recorded datasets. The fit results are summarized in Table I. Again, we define t_s for Fe as 0 fs; for the Ni demagnetization onset, we find 45 fs with a standard error of 24 fs. This comes in almost perfect agreement with the results obtained from T-MOKE. Similar to the T-MOKE data, Fe demagnetizes (about 14%) more than Ni, while demagnetization times are similar for both elements.

As for the discrepancy between our results and earlier XMCD data,[7] like ours the early data sets were obtained by averaging delay scans recorded repeatedly over longer period of times. At the time of the earlier study, the cross correlation technique that we are now using was not available. In Ref. 30, it is mentioned that slow time-zero drifts were corrected for by determining t_0 from Ni and Fe delay scans and by shifting their time axis accordingly. This explains why a temporal offset between Fe and Ni dynamics was not observed.[31]

The experimental XMCD data of this study clearly confirm a delayed demagnetization for Ni in $Fe_{50}Ni_{50}$. Our results provide evidence that the delay found in the demagnetization onset of Ni relative to Fe in the $Ni_{50}Fe_{50}$ alloy is of an intrinsic physical origin. Remarkably, we find even quantitative agreement for the relative-delay: (45 ± 24) fs in XMCD and (45 ± 9) fs in T-MOKE. Given nonlinearity and crosstalk in T-MOKE this agreement is surprisingly good.

As for crosstalk, we observe that the maximum asymmetries for Fe and Ni [Fig. 1(b)] are of similar magnitude. An estimate of the elemental asymmetries from Ref. 24 gives about 20% contribution of Ni asymmetry at the Fe edge for this sample, which would still be sizable. A full optical treatment of T-MOKE of the FeNi alloy, including also cap layers,[32] should be able to quantify the true amount of crosstalk.[33]

Other contributions to non-linearities show quite pronounced energy dependences (also seen dynamically in Ref. 25) but seem less strong near resonance maxima. The deviation in the decay times (t_d) and demagnetization amplitude (m_d) between the two experiments may be assigned to different pump fluence levels. Although we measured shorter decay times for T-MOKE compared to XMCD, the quenching rate (m_d/t_d) turns out to be very similar within the error bars (Table I). The latter is in agreement with findings of Ref. 34.

Our comparative XMCD and T-MOKE study shows that a delay in the Ni demagnetization in $Fe_{50}Ni_{50}$ is an intrinsic effect and not caused by T-MOKE non-linearity or crosstalk issues. The amount of delay observed with both techniques is found to agree remarkably well. With both methods, the amount of demagnetization of the Fe was found to be somewhat larger compared to the Ni. The demagnetization time (t_d) and the amount of demagnetization (m_d) obtained from the XMCD measurements are larger in general compared to that of the T-MOKE measurements, while the quenching rate, m_d/t_d, comes out about the same for both the techniques.

While in this study, T-MOKE results appear reasonably correct, this does not imply that T-MOKE should not be treated with caution—in particular when the involved resonances are close in energy. However, also, $L_{2,3}$-XMCD may need care in time-resolved experiments. Energy dependence seen in EUV-XMCD dynamics experiments suggests that dynamics response at soft x-ray resonances

TABLE I. Results obtained from the fitting of the T-MOKE and XMCD data presented in Figs. 1(b) and 2(b), respectively.

Parameter names	T-MOKE		XMCD	
	Fe	Ni	Fe	Ni
m_d	0.38 ± 0.01	0.30 ± 0.01	0.49 ± 0.01	0.43 ± 0.01
t_d (fs)	221 ± 13	171 ± 15	267 ± 26	256 ± 36
m_d/t_d (ps^{-1})	1.7 ± 0.18	1.8 ± 0.19	1.8 ± 0.21	1.7 ± 0.25
t_s (fs)	0	45 ± 9	0	45 ± 24

may also change across the spectrum. Fortunately, the existing EUV results show that the XMCD signal taken at the energy of largest XMCD contrast is not much affected by energy shifts;[25] we can, hence, expect that our XMCD results should give a reasonably good representation of the time-resolved magnetization even when energy-dependent effects should occur at $L_{2,3}$ resonances as well.

In summary, we verified the hitherto controversially discussed delayed demagnetization of Ni in the FeNi alloy with L_3-XMCD as a different experimental technique. Our experimental study supports the validity of existing theory work and ensures further progress on the field of magnetization dynamics in technologically important multi-element materials.

See the supplementary material for the fitting procedures and results in MoSi-multilayer and estimated recovery times for demagnetization dynamics.

AUTHOR DECLARATIONS
Conflict of Interest

The authors have no conflicts to disclose.

Author Contributions

S.J., C.S.L., and N.P. planned and performed the experiments at the slicing beamline; S. J., R.K., R.S.M., and R.S. performed the experiments at the T-MOKE beamline; S.M. synthesized the samples; and S.J., C.S.L., and N.P. wrote the manuscript with contribution from all the coauthors.

DATA AVAILABILITY

The data that support the findings of this study are available from the corresponding author upon reasonable request.

REFERENCES

[1]W. E. Bailey, L. Cheng, D. J. Keavney et al., "Precessional dynamics of elemental moments in a ferromagnetic alloy," Phys. Rev. B **70**, 172403 (2004).

[2]S. Mathias, C. La-O-Vorakiat, P. Grychtol et al., "Probing the timescale of the exchange interaction in a ferromagnetic alloy," Proc. Natl. Acad. Sci. U. S. A. **109**, 4792–4797 (2012).

[3]S. Günther, C. Spezzani, R. Ciprian et al., "Testing spin-flip scattering as a possible mechanism of ultrafast demagnetization in ordered magnetic alloys," Phys. Rev. B **90**, 180407(R) (2014).

[4]S. Jana, J. A. Terschlüsen, R. Stefanuik et al., "A setup for element specific magnetization dynamics using the transverse magneto-optic Kerr effect in the energy range of 30–72 eV," Rev. Sci. Instrum. **88**, 033113 (2017).

[5]I. Radu, K. Vahaplar, C. Stamm et al., "Transient ferromagnetic-like state mediating ultrafast reversal of antiferromagnetically coupled spins," Nature **472**, 205–208 (2011).

[6]B. Pfau, S. Schaffert, L. Müller et al., "Ultrafast optical demagnetization manipulates nanoscale spin structure in domain walls," Nat. Commun. **3**, 1100 (2012).

[7]I. Radu, C. Stamm, A. Eschenlohr et al., "Ultrafast and distinct spin dynamics in magnetic alloys," SPIN **5**, 1550004 (2015).

[8]E. Turgut, C. La-O-Vorakiat, J. M. Shaw et al., "Controlling the competition between optically induced ultrafast spin-flip scattering and spin transport in magnetic multilayers," Phys. Rev. Lett. **110**, 197201 (2013).

[9]E. Turgut, D. Zusin, D. Legut et al., "Stoner versus Heisenberg: Ultrafast exchange reduction and magnon generation during laser-induced demagnetization," Phys. Rev. B **94**, 220408(R) (2016).

[10]R. Knut, E. K. Delczeg-Czirjak, S. Jana et al., "Inhomogeneous magnon scattering during ultrafast demagnetization," Preprint arXiv:1810.10994 (2018).

[11]S. Jana, R. Knut, E. K. Delczeg-Czirjak et al., "Exchange dependent ultrafast magnetization dynamics in Fe$_{1-x}$Ni$_x$ alloys," Preprint arXiv:1810.11001 (2018).

[12]Y. Pogoryelov, M. Pereiro, S. Jana et al., "Nonreciprocal spin pumping damping in asymmetric magnetic trilayers," Phys. Rev. B **101**, 054401 (2020).

[13]M. Hofherr, S. Häuser, J. K. Dewhurst et al., "Ultrafast optically induced spin transfer in ferromagnetic alloys," Sci. Adv. **6**, eaay8717 (2020).

[14]C. La-O-Vorakiat, M. Siemens, M. M. Murnane et al., "Ultrafast demagnetization dynamics at the M edges of magnetic elements observed using a tabletop high-harmonic soft x-ray source," Phys. Rev. Lett. **103**, 257402 (2009).

[15]C. La-O-Vorakiat, E. Turgut, C. A. Teale et al., "Ultrafast demagnetization measurements using extreme ultraviolet light: Comparison of electronic and magnetic contributions," Phys. Rev. X **2**, 011005 (2012).

[16]C. Stamm, T. Kachel, N. Pontius et al., "Femtosecond modification of electron localization and transfer of angular momentum in nickel," Nat. Mater. **6**, 740–743 (2007).

[17]T. Wang, D. Zhu, B. Wu et al., "Femtosecond single-shot imaging of nanoscale ferromagnetic order in Co/Pd multilayers using resonant x-ray holography," Phys. Rev. Lett. **108**, 267403 (2012).

[18]K. Yao, F. Willems, C. K. Schmising et al., "Distinct spectral response in M-edge magnetic circular dichroism," Phys. Rev. B **102**, 100405 (2020).

[19]C. K. Schmising, F. Willems, S. Sharma et al., "Element-specific magnetization dynamics of complex magnetic systems probed by ultrafast magneto-optical spectroscopy," Appl. Sci. **10**, 7580 (2020).

[20]M. Haag, C. Illg, and M. Fähnle, "Role of electron–magnon scatterings in ultrafast demagnetization," Phys. Rev. B **90**, 014417 (2014).

[21]J. Stöhr and H. C. Siegmann, *Magnetism: From Fundamentals to Nanoscale Dynamics* (Springer, Berlin/Heidelberg, 2006).

[22]P. Carra, B. T. Thole, M. Altarelli, and X. Wang, "X-ray circular dichroism and local magnetic fields," Phys. Rev. Lett. **70**, 694–697 (1993).

[23]C. T. Chen, Y. U. Idzerda, H.-J. Lin et al., "Experimental confirmation of the x-ray magnetic circular dichroism sum rules for iron and cobalt," Phys. Rev. Lett. **75**, 152–155 (1995).

[24]S. Jana, R. S. Malik, Y. O. Kvashnin et al., "Analysis of the linear relationship between asymmetry and magnetic moment at the M edge of 3d transition metals," Phys. Rev. Res. **2**, 013180 (2020).

[25]M. Hennes, B. Rösner, V. Chardonnet et al., "Time-resolved XUV absorption spectroscopy and magnetic circular dichroism at the Ni $M_{2,3}$-edges," Appl. Sci. **11**, 325 (2020).

[26]S. Plogmaker, J. A. Terschlüsen, N. Krebs et al., "HELIOS—A laboratory based on high-order harmonic generation of extreme ultraviolet photons for time-resolved spectroscopy," Rev. Sci. Instrum. **86**, 123107 (2015).

[27]K. Holldack, J. Bahrdt, A. Balzer et al., "FemtoSpeX: A versatile optical pump–soft x-ray probe facility with 100 fs x-ray pulses of variable polarization," J. Synchrotron Radiat. **21**, 1090–1104 (2014).

[28]D. Schick, S. Eckert, N. Pontius et al., "Versatile soft x-ray-optical cross-correlator for ultrafast applications," Struct. Dyn. **3**, 054304 (2016).

[29]S. Jana, S. Muralidhar, J. Åkerman et al., "Using the photoinduced L_3 resonance shift in Fe and Ni as time reference for ultrafast experiments at low flux soft x-ray sources," Struct. Dyn. **8**, 044304 (2021).

[30]A. Eschenlohr, Ph.D. thesis (University of Potsdam, 2012).

[31]We note that correcting t_0 drifts by obtaining the time scale directly from very noisy data may potentially also affect the shape of the averaged data. When aligning scans by, e.g., fitting a decay curve to individual scans. without further precautions the average of such aligned scans can become biased towards either a decay on the time scale of the delay step size or towards the decay shape assumed for the fit.

[32]F. Willems, S. Sharma, C. K. Schmising et al., "Magneto-optical functions at the 3p resonances of Fe, Co, and Ni: *Ab initio* description and experiment," Phys. Rev. Lett. **122**, 217202 (2019).

[33]S. Jana, "Estimating crosstalk in transvers-MOKE at the M edges of transition metals," (to be published) (2022).

[34]B. Koopmans, G. Malinowski, F. Dalla Longa et al., "Explaining the paradoxical diversity of ultrafast laser-induced demagnetization," Nat. Mater. **9**, 259–265 (2010).